Astron. Astrophys. 325, L21–L24 (1997)

ASTRONOMY AND ASTROPHYSICS

LETTER

Letter to the Editor

Infrared spectral energy distributions of the interacting galaxies Arp 244, NGC 6240, and Arp 220⋆

Ulrich Klaas[1,2], **Martin Haas**[1], **Ingolf Heinrichsen**[3,2], **and Bernhard Schulz**[2]

[1] Max-Planck-Institut für Astronomie, Königstuhl 17, D-69117 Heidelberg, Germany,
[2] ISO Science Operations Centre, Astrophysics Division, Space Science Department of ESA, Villafranca, P.O. Box 50727, E-28080 Madrid, Spain
[3] Max-Planck-Institut für Kernphysik, Saupfercheckweg 1, D-69117 Heidelberg, Germany

Received 3 June 1997 / Accepted 26 June 1997

Abstract. For the luminous galaxies Arp 244, NGC 6240 and Arp 220 detailed infrared spectral energy distributions between 3 and 200 μm obtained with ISOPHOT are presented. The maximum of the infrared energy distribution can now clearly be determined. The SEDs can be well represented by cold dust emission with temperatures of 30-50 K which by far dominates the luminosity. In addition, a second warm dust component is present with temperatures of 120-160 K. The infrared luminosities derived from the ISOPHOT data agree, within the errors, with the extrapolated IRAS 8-1000μm luminosities. The cold component of Arp 244 shows similarities to HII regions in normal galaxies, while NGC 6240 and Arp 220 have huge dust masses heated up to considerably higher temperatures. We discuss the observations in the context of heating by starbursts and conversion of mechanical energy from collision or outflow.

Key words: Infrared: galaxies, Galaxies: photometry, fundamental parameters, starburst, individual: Arp 244, NGC6240, Arp 220

1. Introduction

One of the major outcomes of the IRAS mission was the finding of a class of galaxies which emit the bulk of their energy in the far infrared (Soifer et al. 1987). On optical images most of the luminous ones show a peculiar morphology indicating interactions (e.g. Klaas and Elsässer 1993, and for a review Sanders and Mirabel 1996). Sanders et al. (1988) defined the class of ultra-luminous IR galaxies with $L_{FIR} > 10^{12}$ $L_\odot$ and proposed that these objects represent the evolutionary link between starburst galaxies and quasars.

The evolution of the infrared luminous galaxies and the nature of their heating sources are one of the key issues of the coordinated Central Programme of the Infrared Space Observatory (ISO, Kessler et al. 1996; ISOPHOT, Lemke et al. 1996). In this letter we present detailed 3 to 200 μm photometry obtained with ISOPHOT for three classical interacting systems showing increasing interaction strength:

1) Arp 244 (= NGC4038/39), "The Antennae" being the prototype of an interacting system (e.g. Whitmore and Schweizer 1995),
2) NGC 6240, an interacting system with the two nuclei separated by only 2″ (e.g. Fried and Schulz 1983),
3) Arp 220 (= IC 4553), an ultra-luminous merger (e.g. Graham et al. 1990).

2. Observations and Data Reduction

The ISOPHOT observations were performed as part of the observing mode commissioning and of the scientific validation of the off-line processing pipeline (OLP). Therefore, different observing modes (=AOTs, Klaas et al. 1994) were applied and a unique coverage by all 25 ISOPHOT filters was achieved for NGC 6240 and Arp 220.

For Arp 244 the sparse map AOTs PHT17/19 with the largest beam and PHT37/39 were used in order to perform integral photometry of the extended object, whose main body without the tails has a diameter of 3 arcmin in the optical. Exposure times per pointing were 64 s. NGC 6240 and Arp 220 are much more compact, therefore smaller aperture sizes were selected. Typical exposure times for the AOTs PHT03/PHT22 ranged from 32 s

Send offprint requests to: U. Klaas (uklaas@iso.vilspa.esa.es)

⋆ Based on observations with ISO, an ESA project with instruments funded by ESA Member States (especially the PI countries: France, Germany, the Netherlands and the United Kingdom) and with the participation of ISAS and NASA.

Table 1. Pointings of the observations. The on-positions are centred on the objects, the off-positions served for the background subtraction.

Name	Date	RA (2000)	DEC (2000)
Arp 244 on	25 Jan 96	$12^h01^m55^s.1$	$-18°52'43^s$
Arp 244 off	25 Jan 96	$12^h01^m33^s.8$	$-18°52'43^s$
NGC6240 on	06 Mar 97	$16^h52^m58^s.6$	$+02°24'04^s$
NGC6240 off	06 Mar 97	$16^h52^m58^s.6$	$+02°19'04^s$
Arp 220 on	06 Mar 97	$15^h34^m57^s.3$	$+23°30'12^s$
Arp 220 off	06 Mar 97	$15^h34^m57^s.3$	$+23°35'12^s$

in most filters to 128 s in some of the narrow band filters. The on- and off- pointings are listed in Table 1.

The data were reduced using the OLP V6.0 and in parallel the PHT Interactive Analysis (PIA[1]) V6.1 in standard processing mode, together with the calibration data set V3.0 (ISOPHOT Data User Manual V3.0, Laureijs et al. 1997). The results of both software systems were in excellent agreement. The fluxes were corrected for beam size effects of the single pointings. To account for the overall uncertainty in signal derivation as well as relative and absolute photometric calibration we have adopted generally 30% for the errors.

3. Results and Discussion

3.1. Spectral Energy Distributions

The fluxes are listed in Table 2 and the spectral energy distributions are shown in Figure 1. For comparison also the IRAS values are plotted which are in excellent agreement. The remarkable features of the SEDs are:

1) For each galaxy the maximum of the SED can now be very accurately determined. It lies between 70 and 100 μm and the ISOPHOT long wavelength filters clearly outline the Rayleigh-Jeans branch. This branch follows excellently the shape of a modified blackbody with emissivity proportional to λ^{-1} and temperature about 30-50 K. We call this the cold component. For Arp 220 the Rayleigh-Jeans tail is nicely continued by the submm data points measured by Rigopoulou et al. (1996).
2) In addition, shortward of 60 μm there is an excess over the cold component. In order to model the mid infrared SED we fitted a second modified blackbody function with temperature of about 120-160 K. We call it the warm component. Note that the functions are best eye fits and are not simply obtained by least square minimising.
3) For Arp 220 and NGC 6240 shortwards of 20 μm spectral line features appear in addition to the warm component. They include the PAH emission feature at 7.7 μm and the 10 μm silicate absorption, already reported by Smith et al. (1989). Moreover a small emission bump between 12 and 16 μm is present, possibly due to small grains enhanced by the [NeII]12.8 μm and [NeIII] 15.6 μm lines. As Acosta-Pulido et al. (1996) reported this for NGC 6090, it seems to be a common feature in the 12 to 16 μm SEDs of IR luminous galaxies. Note that due to the MIR spectral features the blackbody fit to the warm component is likely to be more uncertain than the fit to the cold component.
4) Between 10 and 60 μm the SED rises much steeper for Arp 220 than for NGC 6240 and Arp 244, or, in other words, the "knee" in the SED at 25 μm is less pronounced for Arp 220.

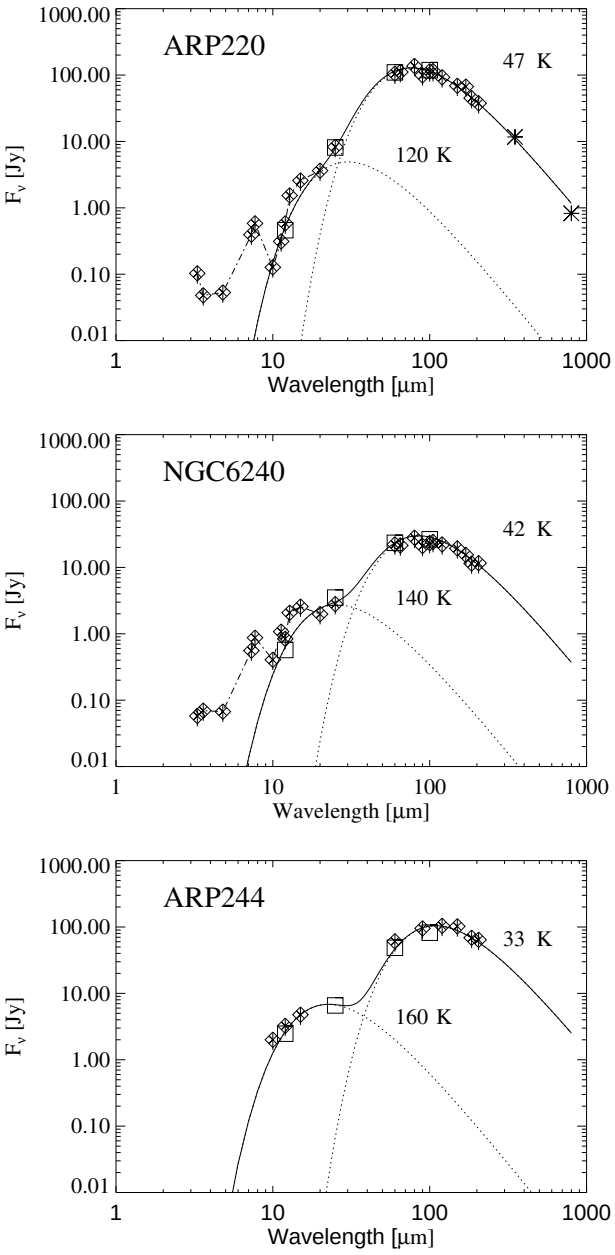

Fig. 1. Spectral energy distributions of Arp 220, NGC 6240 and Arp 244: ◇ ISOPHOT (errors generally adopted to 30%), □ IRAS, ∗ SUBMM (from Rigopoulou et al. 1996), the solid and the dotted lines represent modified blackbody fits with emissivity λ^{-1}, for NGC6240 and Arp220 the dashed-dotted lines connect the ISOPHOT data points in order to emphasize the spectral features shortwards of 20 μm.

[1] PIA is a joint development by the ESA Astrophysics Division and the ISOPHOT Consortium led by the Max Planck Institute for Astronomy (MPIA), Heidelberg. Contributing ISOPHOT Consortium institutes are DIAS, RAL, AIP, MPIK, and MPIA.

Table 2. ISOPHOT photometry.

λ	aperture[a]	Arp 244	NGC 6240	Arp 220	ccf[b]	T_{BB}[c]
[μm]	[arcsec]	[Jy]	[Jy]	[Jy]		[K]
3.3	52		0.058	0.103	-	-
3.6	52		0.070	0.048	-	-
4.8	52		0.067	0.053	-	-
7.3	52		0.557	0.394	-	-
7.7	52		0.872	0.583	-	-
10.0	52	2.00	0.406	0.127	-	-
11.3	52		1.08	0.312	-	-
12.0	52	3.25	0.839	0.583	0.95	100
12.8	52		2.08	1.54	1.00	100
15.0	52	4.78	2.57	2.58	1.01	100
20.0	79		1.98	3.63	0.94	100
25.0	79		2.80	8.28	1.04	100
60.0	180		17.4	88.7	0.96	40
60.0	138x138	60.9	22.2	105.0	0.96	40
65.0	138x138		21.4	111.0	0.97	40
80.0	138x138		28.0	137.0	1.09	40
90.0	138x138	95.2	21.0	99.0	1.04	40
100.0	180		23.1	95.6	1.04	40
100.0	138x138		23.2	113.7	1.08	40
105.0	138x138		24.2	114.4	1.04	40
120.0	184x184	104.1	22.2	92.5	1.26	40
150.0	184x184	102.3	19.4	69.0	1.18	40
170.0	184x184		15.4	67.0	1.40	40
180.0	184x184	68.8	11.4	45.0	1.20	40
200.0	184x184	64.1	11.6	37.6	1.08	40

[a] P1, P2 and P3 data (3-100 μm) for NGC 6240 and Arp 220 are denoted by a single aperture value (diameter), C100 and C200 data (60-200 μm) by the array area. For the extended galaxy Arp 244 the PHT-P fluxes refer to a 180″ aperture.

[b] Colour correction factors *ccf* for a modified blackbody spectrum proportional to ν B(ν,T_{BB}) for $\lambda \geq 12$ μm. The fluxes quoted in columns 3-5 are yet uncorrected, for a detailed modelling division by the color correction factors may be necessary.

[c] Temperature of the modified blackbody for which the *ccf* are given.

This may be the consequence of increasing extinction from Arp 244 over NGC 6240 to Arp 220, as discussed by Lutz et al. (1996).

In particular for NGC 6240 and Arp 220 we have obtained the most detailed infrared spectral energy distributions which can better constrain galaxy dust models. Note that the fluxes quoted in Table 2 refer to a spectral shape of $\nu F_\nu = const$ passing the filter and detector bands. As this is not the real spectral energy distribution for our galaxies, for a detailed modelling it might be necessary to apply color corrections. Therefore color correction factors for a modified blackbody spectrum proportional to ν B(ν,T), which is a good first order approximation, are given in Table 2. In the following we will confine to the simplest dust model and discuss the observed spectral energy distribution fitted with two modified blackbody functions. We did not apply any color correction, because the effect is small and it does not influence our basic results.

Table 3. IR flux obtained from IRAS and ISOPHOT using various wavelength ranges. For more details of PHT_{BB} see Table 4. The fluxes are given in [10^{-14} Wm^{-2}].

Name	PHT 8-130μm	PHT 3-220μm	PHT_{BB} 1-1000μm	IRAS[a] 8-1000μm
Arp 244	420	511	499	491
NGC 6240	154	180	179	201
Arp 220	576	637	725	770

[a] $F_{IR} = 1.8 \cdot \{ 13.48\, f_{12} + 5.16\, f_{25} + 2.58\, f_{60} + f_{100} \}$ [10^{-14} Wm^{-2}] (see Sanders and Mirabel, 1996)

3.2. Luminosities, dust temperatures and masses

In Table 3 the first two columns PHT_{8-130} (= the IRAS range) and PHT_{3-220} (= the ISOPHOT range) list the IR flux contributions in synthetic non-overlapping bandpasses. Column 3 (PHT_{BB}) gives the integrated flux between 1 and 1000 μm derived from the blackbodyfits. In column 4 we give for comparison the extrapolated mid and far infrared flux according to the definition in Table 1 of Sanders and Mirabel (1996). The main results of this comparison are:

1) Including the far infrared capabilities of ISOPHOT beyond 100 μm shows that the additional flux amounts to about 10% for Arp 220, 15% for NGC6240 and 18% for Arp 244.
2) Assuming that the PHT_{BB} gives the best estimate of the total flux, the IRAS range comprises already 80-90% and the ISOPHOT range 90-100%.
3) While for Arp 244 and NGC 6240 the PHT_{3-220} fluxes correspond well with the total flux from 1-1000 μm, a considerably smaller 3-220 μm flux is derived for Arp 220. This flux deficit can be explained by the coarse wavelength coverage between 25 and 60 μm which underestimates the flux due to the steep rise of the Arp 220 SED.
4) The IRAS extrapolation and the double blackbody fit results agree well within the adopted error range.

From the blackbody fits we derive the IR luminosity contributions between 1 and 1000 μm for the cold and warm component, respectively (H_0 = 75 km/sec/Mpc). They are given in Table 4 together with their sum. Note that the total luminosities are dominated by the cold component.

The dust masses of the cold and warm components are compiled in Table 4, derived from the luminosities and dust temperatures using the formula given in Klaas and Elsässer (1993). E.g. for ARP 220 our estimate agrees within the errors with that obtained by Scoville et al.(1991) from IRAS and submm data ($M_{dust} = 5 \cdot 10^{10}$ [$M_\odot$]). For comparison Table 4 also lists the gas masses from the literature. The dust-to-gas ratio lies about 1/300, a factor of three lower than the standard galactic dust-to-gas ratio.

The sequence Arp 244 - NGC 6240 - Arp 220 exhibits significant trends, the cold component showing an increase in luminosity, temperature and mass. The warm component, surprisingly, shows an apparent decrease in temperature, probably the consequence of increasing extinction mentioned above. In Arp

Table 4. Infrared luminosities (1-1000 μm), dust temperatures and masses derived from two modified blackbodies with emissivity λ^{-1} (H_0 = 75 km/sec/Mpc). For comparison also the total molecular gas masses M(H_2) are listed.

Name	**Flux**$_{\rm cold+warm}$ [10^{-14} W/m^2]	**D** [Mpc]	**L**$_{\rm cold+warm}$ [L$_\odot$]	**L**$_{\rm cold}$ [L$_\odot$]	**L**$_{\rm warm}$ [L$_\odot$]	**T**$_{\rm cold}$ [K]	**T**$_{\rm warm}$ [K]	**M**$_{\rm cold}$ [M$_\odot$]	**M**$_{\rm warm}$ [M$_\odot$]	**M(H$_2$)** [M$_\odot$]
Arp 244	499.0	21.0	6.43e+10	4.87e+10	1.55e+10	33	160	1.27e+7	1.52e+3	3.9e+9[a]
NGC 6240	178.9	98.0	5.02e+11	3.83e+11	1.18e+11	42	140	3.00e+7	2.25e+4	10.8e+9[b]
Arp 220	724.8	72.9	1.13e+12	1.02e+12	1.01e+11	47	120	4.57e+7	4.16e+4	14.4e+9[b]

[a] from Sanders and Mirabel 1996

[b] from Solomon et al. 1997 (gas mass assumed to be equal to the dynamical mass)

244 a relatively small dust mass amounts to a significant fraction of the IR luminosity. In Arp 220 nearly the whole luminosity is generated by the cold component, though the strong extinction could displace the ratio against the warm component.

3.3. Heating of the cold and warm component

Arp 244: The temperature of the cold dust component is close to that found for normal spirals (M101) or weakly interacting objects (M51), even including HII-regions (e.g. Hippelein et al. 1996). The bimodal appearance of the SED is similar to that of Seyfert galaxies, where the warm component is interpreted as being powered by the active nucleus (Rodriguez Espinosa et al. 1996). This mechanism, however, can be ruled out for Arp 244. Spatially resolved IR imaging between 12 and 18 μm by Vigroux et al. (1996) shows that the main activity is taking place in a few hot spots in the overlap region of the two galaxy disks and not in the nuclei.

NGC 6240 and Arp 220: In these tightly interacting and merging systems huge dust masses (3 to 5 $\cdot$ 10^7 M$_\odot$) are efficiently heated to temperatures 10 – 20 K higher than found in normal galaxies. Although for Arp 220 a large fraction of the molecular gas mass is concentrated within a very small region, the derived dust parameters argue for more spatially extended heating sources. It could be direct heating by a starburst as suggested by Lutz et al. (1996). Also the prominent PAH features argue against an AGN as the only heating source. The optical spectra of both objects are LINER types (Fried and Ulrich 1985, Sanders et al. 1988). NGC 6240 is the most luminous source of 1–0 S(1) H_2 emission indicative for shocks (Goldader et al. 1997), and extended X–ray emission has been found for Arp 220 (Heckman et al. 1996). Therefore, collision of clouds similar to a model proposed by Harwit et al. (1987) or bipolar superwinds (Heckman et al. 1990) could be responsible for heating up a large mass of the ISM. For Arp 220 many typical features of an AGN are reported, too (Sanders and Mirabel 1996). An AGN could therefore power the warm component.

Acknowledgements. It is a pleasure for us to thank our collegues of the ISOPHOT Instrument Dedicated Team in Vilspa and the ISOPHOT Data Centre in Heidelberg for their extreme engagement in the scientific validation and calibration of the instrument. We also thank the ISO Project Scientist Martin Kessler for granting special observing time for the OLP validation. For literature search and IRAS photometry we used the NASA/IPAC Extragalactic Data Base (NED) and the NASA Astrophysics Data System (ADS). We thank the referee for constructive comments.

References

Acosta–Pulido J.A., Klaas U., Laureijs R.J., et al., 1996, A&A 315, L21
Fried J., Schulz H., 1983, A&A 118, 166
Fried J., Ulrich H., 1985, A&A 152, L14
Goldader J.D., Joseph R.D., Doyon R., Sanders D.B., 1997, ApJ 474, 107
Graham J.R., Carico P., Matthews K., et al., 1990, ApJ 354, L5
Harwit M., Houck J.R., Soifer B.T., Palumbo G.G.C., 1987, ApJ 315, 28
Heckman T.M., Armus L., Miley G.K., 1990, ApJ Suppl. 74, 833
Heckman T.M., Dahlem M., Eales S.A., Fabbiano G., Weaver K., 1996, ApJ 457, 616
Hippelein H., Lemke D., Haas M., et al., 1996, A&A 315, L82
Kessler M.F., Steinz J.A., Anderegg M.E., et al., 1996, A&A 315, L27
Klaas U., Elsässer H., 1993, A&A 280, 76
Klaas U., Krüger H., Heinrichsen I., Heske A., Laureijs R., 1994, "ISOPHOT Observers Manual, Version 3.1"
Laureijs R. et al., 1997, ISOPHOT Data User Manual, V3.0
Lemke D., Klaas U., Abolins J., et al., 1996, A&A 315, L64
Lutz D., Genzel R., Sternberg A., et al., 1996, A&A 315, L137
Rigopoulou D., Lawrence A., Rowan-Robinson M., 1996, MNRAS 278, 1049
Rodriguez-Espinoza J.M., Perez Garcia A.M., Lemke D., Meisenheimer K., 1996, A&A 315, L129
Sanders D.B., Mirabel I.F., 1996, ARAA 34, 749
Sanders D.B., Soifer B.T., Elias J.H., et al., 1988, ApJ 325, 74
Scoville N.Z., Sargent A.I., Sanders D.B., Soifer B.T., 1991, ApJL 366, L5
Smith C.H., Aitken D.K., Roche P.F., 1989, MNRAS 241, 425
Soifer B.T., Houck J.R., Neugebauer G., 1987, ARAA 25, 187
Solomon P.M., Downes D., Radford S.J.E., Barrett J.W. 1997, ApJ 478, 144
Vigroux L., Mirabel F., Altieri B., et al., 1996, A&A 315, L93
Whitmore B.C., Schweizer F., 1995, AJ, 109, 960

This article was processed by the author using Springer-Verlag LaTeX A&A style file *L-AA* version 3.